Macroscopic Model for Predicting Columnar to Equiaxed Transitions using Columnar Front Tracking and Average Equiaxed Growth

Wajira U. Mirihanage[1,a], Shaun McFadden[1] and David J. Browne[1,b]

[1]School of Electrical, Electronic & Mechanical Engineering,
University College Dublin, Belfield, Dublin 4, Ireland.
[a]wajira.mirihanage@ucd.ie [b]david.browne@ucd.ie

Keywords: Solidification, CET, Equiaxed growth

Abstract. A macroscopic model of Columnar-to-Equiaxed Transition (CET) formation is presented. The growth of a columnar zone and an equiaxed zone are treated separately and modeled on a fixed grid. The model uses a columnar Front Tracking (FT) formulation to compute the motion of the columnar front and the solidification of the dendritic columnar mushy zone. The model for the equiaxed zone calculates the average growth of equiaxed grains within the control volumes of undercooled liquid. The proposed model, which calculates the average equiaxed growth, is different from previous FT models which consider each equiaxed grain envelope separately. A lognormal size distribution model of seed particles is used for the equiaxed nucleation in the undercooled liquid zone. After nucleation, average equiaxed growth is computed by considering the equiaxed envelopes as spherical. The extended volume concept is used to deal with grain impingement. The Scheil equation is used to calculate the solid fraction and latent heat release. When the equiaxed fraction is great enough, advancement of the columnar front is halted and the CET position is determined. CET formation was simulated for directional solidification of an aluminium-silicon alloy. The results were compared with a previous FT-CET prediction model as well as with experimental data. Agreement was found in both cases.

Introduction

When columnar and equiaxed zones co-exist in a casting, a distinguishable transition is called the Columnar-to-Equiaxed Transition (CET). Over the years much research attention has been given to analytical, experimental and computer modelling of CET. Recently, Spittle [1] reviewed CET analysis. In other work, McFadden and Browne [2,3] presented a Front Tracking (FT) model to predict CET in alloy casting. CET models have been proposed at various scales [3-9]. Mechanical blocking [4] or solutal blocking [5] mechanisms are mostly used to halt the columnar growth and to define the CET position.

The model presented here follows the equiaxed heterogeneous nucleation in the liquid ahead of growing solid/liquid interface. As an initial development, solutal interactions near impingement are not considered. In the present work, a FT model presented by Browne and Hunt [10, 11], which was later extended by McFadden and Browne [3], is used to compute the growth of the columnar zone. The proposed model does not track crystallographic or microscopic details for each dendrite, thus reducing the computational overhead considerably. A model, presented by Jacot et al.[8] has common features with this model in terms of growth and impingement of equiaxed grains.

This volume-averaging approach to equiaxed solidification is being developed here because it will facilitate the integration of the effects of convection into the model, at low computational overhead, in comparison to the need to track flow between and motion of the individual equiaxed grains directly simulated in [3]. The aim of the current contribution is verification and validation of the new model of equiaxed nucleation, growth and impingement and CET criteria in diffusion-controlled solidification.

The Model

The FT model is used to simulate the advancement of the columnar zone and the development of undercooling in the liquid zone ahead of it. Four different zones can be identified (fig.1): solid, columnar mush, equiaxed mush in undercooled liquid, and superheated liquid.

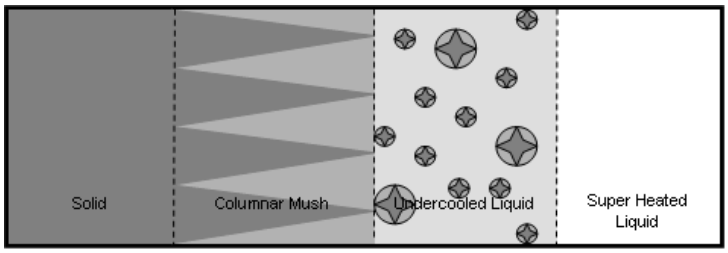

Fig.1 Solid, columnar mush, equiaxed mush in undercooled liquid and superheated liquid.

The heat equation, equation (1) is explicitly solved in a fixed grid and a control volume (CV) approach is used for model calculations.

$$\rho C_p \frac{\partial T}{\partial t} = \nabla \left(K \nabla T \right) + E \qquad (1)$$

Where ρ is the density, K is the thermal conductivity; C_p is specific heat; T and t denote the temperature and time, respectively, and E is the source term associated with latent heat evolution.

Columnar Zone and Equiaxed Zones. The columnar FT model is presented elsewhere [10,11] and not detailed in this contribution. There are two basic requirements [9] for formation of an equiaxed zone; those are, the presence of active nuclei ahead of columnar front and favourable conditions promoting their growth. The presence of inoculants, impurities, or fragmented dendrite arms, and the availability of an undercooled liquid zone ahead of the columnar front, satisfy these requirements. Equiaxed nucleation and growth are discussed in subsequent sections.

Equiaxed Nucleation. Nucleation begins from available seed particles. Uniform distribution of those seeds in undercooled liquid is assumed. Equiaxed crystal nucleation depends on the seed particles' geometry as discussed by Greer et al. [13]. For nucleation from an inoculation particle, this barrier to nucleation is overcome at the initiation undercooling ΔT_i.. Initiation undercooling is related to the diameter d of the seed particle. The relationship is given by equation (2), where, ΔS_V is the volumetric entropy of fusion and γ is the solid-liquid interfacial energy.

$$\Delta T_i = \frac{4\gamma}{\Delta S_v d} \qquad (2)$$

The initiation undercooling is the condition required for free growth of the crystal from the seed particles [14]. Only one possible nucleation from one seed particle is assumed. According to Quested and Greer [14], the size distribution of seed particles follows a lognormal distribution, which we use in this model.

The probabilistic density function *P(d)* for a lognormal distribution is defined as,

$$P(d) = \frac{1}{\sigma d \sqrt{2\pi}} \exp\left(- \frac{(\ln d - \ln \mu)^2}{2\sigma^2} \right) \quad (3)$$

Where, σ and μ are relevant to the standard deviation and the geometric mean.
For a given undercooling, the critical diameter for free growth or initiation of the equiaxed dendrite is calculated. When that undercooling is reached, all the inoculant particles of diameter above critical start to nucleate. In the model, the critical diameter at the local temperature is computed at each time step and all inoculants particles above that diameter (which have not nucleated previously) are then activated for nucleation. In this way nucleation is continued until the control volume is completely occupied by the equiaxed envelopes or the columnar front.

Equiaxed Envelope Growth and Impingement. Dendrite tip velocity is calculated according to relationship in ref.[15]. A low thermal gradient is assumed and the following modified equation is used to calculate dendrite tip velocity, v_t at undercooling ΔT_t,

$$v_t = C.\Delta T_t^{\,n} \quad (4)$$

Here, C is the growth coefficient and n is constant. The resultant dendrite tip advancement Z_t in Δt time is given by,

$$Z_t = v_t.\Delta t \quad (5)$$

The hypothetical sphere that wraps around the dendrite tips is defined as the computational spherical equiaxed mushy envelope, which contains the interdendritic liquid and the solid dendrite. Growth of these hypothetical mushy envelopes is computed as equation (5) provides the increment of radius in each time step.
The average size of all the nucleated envelopes is computed by averaging the diameters of newly nucleated envelopes and existing equiaxed mushy envelopes. To consider grain impingement, the sum of all envelopes is taken as the extended volume $\phi_{ext.}$ [16]. Hence, the net volume fraction of the equiaxed mushy envelops ϕ, is calculated by.

$$\phi = 1 - \exp\left[-\phi_{ext} \right] \quad (6)$$

Latent Heat and Solid Fraction. Latent heat release due to equiaxed and columnar solidification is incorporated into the model. The contributions to latent heat releases come from expansion of mushy envelopes as well as thickening dendrites within each envelope as described in refs.[3,10,11]. Assuming no solute back diffusion in the solid phase and complete mixing of solute in the liquid phase between dendrite arms, the Scheil approximation is used to calculate solid faction, g_s. During the eutectic solidification solid fraction change is computed by considering the enthalpy, H. Complete solid fraction calculation in different temperature intervals is described in equation(7). Here T_L, T_E, T_M, k and L are equilibrium liquidus temperature, eutectic temperature, melting temperature of pure solvent material, partition coefficient and latent heat liberated for unit mass of the alloy, respectively. The Scheil equation gives a reasonable approximation to the solidification path between the T_L and T_E, because a negligible amount of solute leaves the envelope during dendritic growth in diffusive conditions[3]. Equation(9) for isothermal eutectic freezing follows the conservative enthalpy method as proposed in [17]. g_{Scheil} and $g_{eutectic}$ in eq(7) are given by eq.(8) and (9), respectively,

$$g_s = \begin{cases} 0 & \forall \quad T \geq T_L \\ g_{Scheil} & \forall \quad T_L > T > T_E \\ g_{eutectic} & \forall \quad T = T_E \\ 1 & \forall \quad T < T_E \end{cases} \tag{7}$$

$$g_{Scheil} = 1 - \left[\frac{T_M - T}{T_M - T_L} \right]^{\frac{1}{k-1}} \tag{8}$$

$$g_{eutectic} = 1 - \frac{H - C_p T_E}{L} \tag{9}$$

CET Position. The evolution of equiaxed and columnar solid fraction in each CV is separately calculated by coupling the equiaxed model with the columnar growth model. When equiaxed grain envelopes fully occupy a CV (equiaxed grain fraction=1.0), columnar growth is halted locally and no further growth of the columnar front is allowed. A similar halting mechanism with an equiaxed grain fraction of unity was cited previously in ref.[18]

Results and Discussion

Comparisons with a previous model. Numerical simulation using the model is carried out for directional solidification of an Al-7wt.%Si alloy. The simulation followed the conditions of experiments performed by Gandin [19] and used thermophysical data from ref. [15]. The inverse heat transfer technique used to reconstruct the heat flux in the model is described in ref. [3].

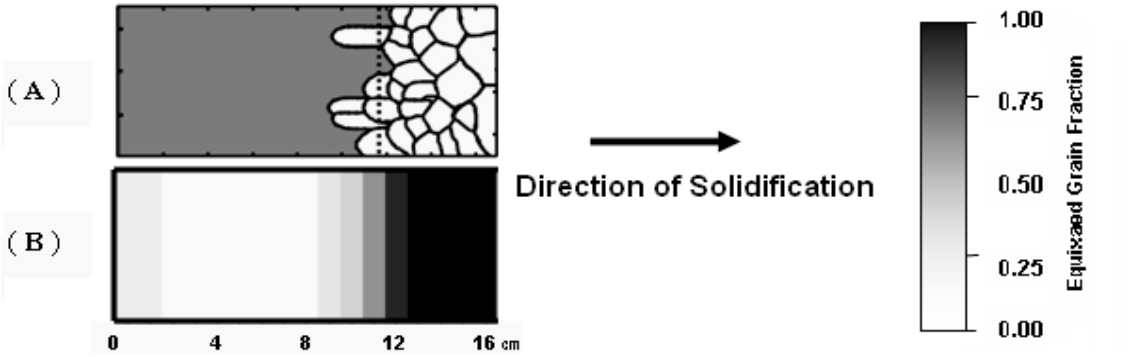

Fig. 2 Comparison of FT model predictions [3] of McFadden and Browne (A) with current predictions (B)

No input seed data was available from the experiments, so 100 uniformly distributed seeds were used in the simulation as per McFadden and Browne [3]. The simulation result was compared with the predictions of the FT-CET model of McFadden and Browne [3]. Fig.2 shows this comparison. Figure 2.A shows the result from [3], where the columnar zone is shown in grey and the equiaxed grains are in white. Figure 2.B shows the results from the current model, where the volume fraction of equiaxed grains is shown in grey scale. In Fig 2.B the extreme right side is fully equiaxed while left side is fully columnar. Judging by the grey scale, the transition zone is started around 10cm from the left edge and at 13 to 14cm it becomes fully equiaxed. According to the macrographs obtained from the McFadden and Browne's model simulation (Fig. 2.A), equiaxed grains were formed at

10cm from left edge of the mould. But, such grains are elongated until a distance of 13-14cm. From that point onwards it is possible to observe equiaxed grains with near-equal height to width ratio. Both models used exactly the same conditions and same thermophysical data. Notably, both used the same FT model to track the advancement of the columnar front. Therefore the new deterministic equiaxed model shows reasonable agreement with the FT equiaxed model [3]. This current model has been verified against a previous model.

Comparisons with the experimental results. The predictions in ref. [3] showed good agreement with the CET position, but not with the observed equiaxed grain size. Therefore, the number of the uniformly distributed seed particles was increased to 750, which gives the close match for grain size of reported experimental results [5]. The simulation was repeated. Then, the fully equiaxed zone started at a distance of 12cm from the left edge (Fig. 3.A). The CET results are in reasonable agreements with the CET position of the experiment [19]; 11.8 cm from the bottom of the mould, which is the chill-end of the experimental set up, shown as the left-hand side here. According to the experiments [19] no columnar grains are visible beyond 11.8 cm from chill-end.

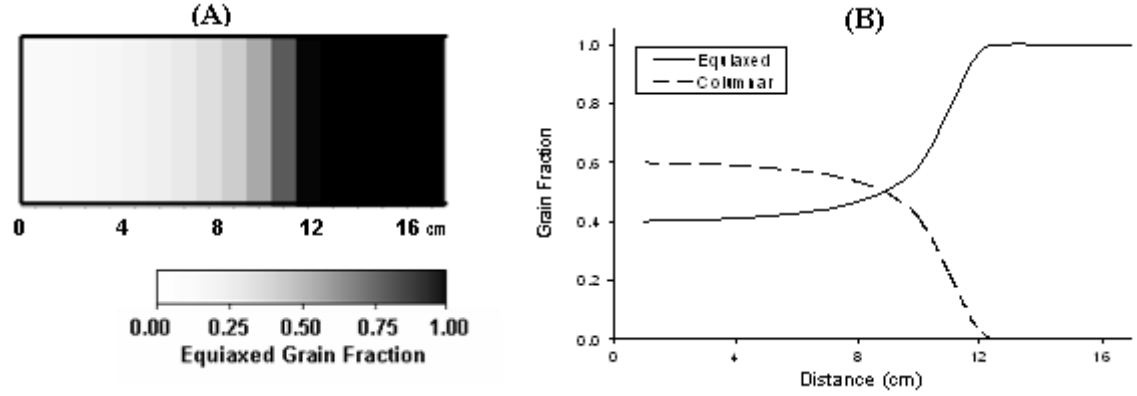

Fig. 3 Simulation results with 750 uniformly distributed seeds

The average equiaxed grain diameter is calculated by using average equiaxed grain densities, which are predicted from the simulation (table1). The agreement between predicted average equiaxed grain diameter and experimental data (5mm avg. diameter, as given in [5] for Al-7%Si alloy; half space - R_f = 2.5 mm) is also good.

Table 1. Simulated grain density and diameter of the equiaxed zone

Distance [cm] from left edge	12-13	13-14	14-15	15-16	16-17
Grain Density [/cm^2]	5.213	5.223	5.232	5.241	5.249
Grain Diameter [mm]	4.94	4.94	4.93	4.93	4.93

According to the simulation results it is possible to see moderate fraction of equiaxed grains even at the columnar region. Even though the exact experimental data is not available, a very low amount of equiaxed grains are visible close to the bottom of the mould in the Al-7%Si micrograph in ref. [19]. That experiment was carried out without purposely added inoculants. In such conditions, very low initial seed density is expected in the melt. Later, when columnar dendrites grow further into the undercooled melt, the nucleation seed density could be increased by provision of additional nucleation sites to the melt to represent possible phenomena such as dendrite tip re-melting and fragmentation [20] etc.. But the current model simulation is performed with a constant and uniform distribution of seeds throughout the melt, which may be accurate for grain-refined

experiments. It is possible that the imposed seed density matches the experimental one at a distance of more then 12 cm from chill-end, as solidification progresses. But because the starting computational seed density is higher than in reality, in the simulation we have excessive equiaxed nucleation potential at early stages (close to the chill-end) of solidification. This could be the main reason for prediction of higher equiaxed grain fraction in the material solidified at initial stage of the solidification process.

Conclusion

The macroscopic CET model is described. The new model is different from previous FT stochastic models and is computationally efficient when convection effects are integrated [21]. This deterministic model predicts the columnar and equiaxed grain fractions with average equiaxed grain size. Reasonable agreement was found between the model simulations and the experimental results.

Acknowledgments

The authors wish to acknowledge the support of European Space Agency (ESA) under ~~the~~ PRODEX funding (contract 90267). This work is part of the ESA-MAP project CETSOL.

References

1. Spittle J.A., Inter. Materials Reviews, 2006, vol 51; no: 4, pp 247-269
2. McFadden S., PhD Thesis, 2007, University College Dublin-Ireland
3. McFadden S., Browne D.J., Appl. Math. Modell., 2009, 33, pp 1397-1416
4. Hunt J.D., Mater. Sc. Eng., 1984, vol 65, pp 73-83
5. Martorano M.A.,Beckermann C.,Gandin Ch-A., Metal.Mater.Trans. 2003,34A,1657-74
6. Rappaz M., Gandin Ch-A., Acta Metall. 1989, 23, pp.1777
7. Wang C.Y., Beckermann C., Metall. Mater. Trans. A; 1996, vol 27A, pp 2755-64
8. Jacot A., Maijer D., Cockcroft S., Metall. Mater. Trans. A, 2000, 31A, pp 2059-68
9. Flood S.C., Hunt J.D., J. Cryst. Growth, 1987, 82, pp 552-560
10. Browne D.J., Hunt J.D., Modeling of Casting, Welding and Advanced Solidification Processes IX, Edited by Sahm P.R., Hansen P.N., Conley J.G., Aachen, Germany, 2000, pp. 437-444
11. Browne D.J., Hunt J.D., Num. Heat. Trans. B, 2004, 45, pp 395-419
12. Burden M.H., Hunt J.D., J. Cryst. Growth, 1974, 22, pp 109-116
13. Greer A.L., Bunn A.M, Tronche A., Evans P.V., Bristow D.J., Acta Mater., 2000, 48, pp 2823–35,.
14. Quested T.E., Greer A.L., Acta Mater., 2005, 53, pp 4643-53
15. Gandin Ch.-A., Acta Mater., 2000, 48, pp 2483–2501
16. Christian J.W., Theory of Transformations in Metals and Alloys, Pergamon, Oxford, 1975, p 17
17. Voller V.R., Advances in Numerical Heat Transfer eds. Minkowycz W.J., Sparrow E.M., vol 1, Taylor and Francis, 1997, pp 341-380
18. M'Hamdi M.,Bobadilla M.,Combeau H.,Lesoult G., in proceedings of Welding and Advanced Solidification Processes VIII, Edited by Thomas B.G. and Beckermann C., The Minerals, Metals & Metals Society, 1998, pp 375-82
19. Gandin Ch.-A., ISIJ Int., 2000, 40, pp 971–979
20. Jackson K.A., Hunt J.D., Uhlmamm D.R., Seward T.P., Trans.of Metall. Soc.of AIME, 1966, vol. 236, pp 140 -158
21. Mirihanage W.U., McFadden S., Browne D.J., 3rd Int. Shape Casting Symposium (TMS Annual Meeting) edited by J. Campbell, P.N. Crepeau, M. Tiryakioglu, 2009, pp.257-263